

## Beta-decay of $^{56}\text{Cu}$

M. Ramdhane <sup>a</sup>, P. Baumann <sup>a</sup>, A. Knipper <sup>a</sup>, G. Walter <sup>a</sup>, Z. Janas <sup>b</sup>, A. Płochocki <sup>b</sup>,  
J. Äystö <sup>c</sup>, P. Dendooven <sup>c</sup>, A. Jokinen <sup>c</sup>, M. Oinonen <sup>c</sup>, H. Penttilä <sup>c</sup>, W. Liu <sup>d</sup>,  
M. Górska <sup>b,d</sup>, H. Grawe <sup>d</sup>, Z. Hu <sup>d</sup>, R. Kirchner <sup>d</sup>, O. Klepper <sup>d</sup>, E. Roeckl <sup>d</sup>,  
Y. Fujita <sup>e</sup>, B.A. Brown <sup>f</sup>

<sup>a</sup> Institut de Recherches Subatomiques, F-67037 Strasbourg, France

<sup>b</sup> Institute of Experimental Physics, Warsaw University, PL-00681 Warsaw, Poland

<sup>c</sup> University of Jyväskylä, FIN-40351, Finland

<sup>d</sup> Gesellschaft für Schwerionenforschung, D-64220 Darmstadt, Germany

<sup>e</sup> Osaka University, Osaka 560, Japan

<sup>f</sup> Michigan State University, East Lansing, MI 48824, USA

Received 17 February 1998; revised 6 May 1998

Editor: R.H. Siemssen

### Abstract

By measuring positrons and  $\beta$ -delayed  $\gamma$ -rays emitted from mass-separated sources, the decay of  $^{56}\text{Cu}$  ( $4^+, T_z = -1, T = 1$ ) to states in the doubly-magic nucleus  $^{56}\text{Ni}$  was studied for the first time. The half-life of  $^{56}\text{Cu}$  was measured to be 78(15) ms, and four  $\beta$ -delayed  $\gamma$ -rays were assigned to its decay. The resulting experimental data on Fermi and Gamow-Teller strength are compared with shell-model predictions. © 1998 Elsevier Science B.V. All rights reserved.

PACS: 23.40.-s; 23.40.z; 27.40.+z; 21.60.Cs

Keywords: Radioactivity  $^{56}\text{Cu}$  [from  $^{nat}\text{Si}(^{32}\text{S}, \text{xpyn})$ ]; Measured  $E_\gamma$ ,  $I_\gamma$ ,  $T_{1/2}$ ; Deduced  $\log ft$ ,  $J^\pi$ ; On-line mass separation; Ge-detectors; Plastic-scintillator detector; Nuclear structure  $^{56}\text{Ni}$ ,  $^{56}\text{Cu}$ ; Calculated levels; Gamow-Teller strength; Shell model

### 1. Introduction

There has been considerable recent progress in reaction studies of the doubly magic ( $N = Z = 28$ ) nucleus  $^{56}\text{Ni}$  and of neighbouring (single-particle) nuclei. One example is the measurement of the transition probability to the first excited state of  $^{56}\text{Ni}$  [1], another one is the investigation of the neutron transfer reaction  $d(^{56}\text{Ni}, p)^{57}\text{Ni}$  [2]. The latter data, together with those on excited states of  $^{57}\text{Cu}$  deduced from  $p(^{58}\text{Ni}, 2n)^{57}\text{Cu}$  work [3], have been used

to estimate the astrophysically interesting  $^{56}\text{Ni}(p, \gamma)^{57}\text{Cu}$  rate. The region of  $^{56}\text{Ni}$  is also a recent focus of the new Quantum Monte Carlo methods for carrying out  $fp$  shell-model calculations [4,5].

In comparison to this impressive progress, the advance of  $\beta$ -decay studies near  $^{56}\text{Ni}$  has been rather modest, even though such measurements for  $^{56}\text{Ni}$  or single-nucleon configurations in its neighborhood are of great interest for tests of predictions of the Gamow-Teller (GT) strength  $B(GT)$ . In addi-

tion to the genuine interest in GT transitions and their quenching in heavy nuclei, these tests and the related improvements of models are in turn linked to the reaction physics and astrophysics questions mentioned above.

The  $\beta$ -decay of the nucleus  $^{56}\text{Ni}$  itself is hampered by the small  $Q_{EC}$  value of 2135(11) keV [6]. Correspondingly, only one GT transition is energetically possible, i.e. that to the first excited  $1^+$  state in  $^{56}\text{Co}$ , whereas the coupling to higher-lying  $1^+$  levels cannot be explicitly probed in  $\beta$ -decay. However, related GT decays can be studied by investigating  $\beta$ -decay of single-nucleon configurations such as the one  $\nu$ -hole or one  $\pi$ -particle nuclei  $^{55}\text{Ni}$  ( $7/2^-, T_z = -1/2, T = 1/2$ ) and  $^{57}\text{Cu}$  ( $3/2^-, T_z = -1/2, T = 1/2$ ), respectively, or the one  $\nu$ -hole, one  $\pi$ -particle nucleus  $^{56}\text{Cu}$  ( $4^+, T_z = -1, T = 1$ ). In all three cases, the  $Q_{EC}$  values are unusually high and the “decay window restriction” is thus considerably less severe than for  $^{56}\text{Ni}$ : Experimental  $Q_{EC}$  results of 8694(11) and 8771(16) keV have been reported [6] for  $^{55}\text{Ni}$  and  $^{57}\text{Cu}$ , respectively, whereas the  $Q_{EC}$  value of  $^{56}\text{Cu}$  has been calculated from Coulomb energy differences to be 15300(140) keV [6] or 15307(67) keV [7]. A further attractive feature of the decay of  $^{56}\text{Cu}$  is that *several* GT transitions should rather easily be accessible and distinguishable from the superallowed Fermi transition. This is in contrast to the cases of  $^{55}\text{Ni}$  ( $T_{1/2} = 207(5)$  ms [6]) and  $^{57}\text{Cu}$  ( $T_{1/2} = 196.3(7)$  ms [6]) whose disintegration is dominated by a mixed Fermi and GT  $\beta$ -decay to the daughter ground states.

$^{56}\text{Cu}$  has first been observed as a product of intermediate-energy  $^{58}\text{Ni} + ^{\text{nat}}\text{Ni}$  projectile–fragmentation reactions [8]. However, this identification experiment does not yield any nuclear structure information except for a lower limit of the order of 200 ns for the half-life of  $^{56}\text{Cu}$ . The problem of studying the  $\beta$ -decay of this nucleus is that its production rate in the most suitable reactions, i.e. those based on fragmentation or fusion–evaporation reactions, is small, in particular if the limited transmission of the experimental device, which generally is a magnetic spectrometer or an isotope separator on-line (ISOL), is taken into account. Furthermore, due to the large  $Q_{EC}$  value and the combined action of F and GT transitions, its half-life is expected to be short, i.e. of the order of 100 ms.

We report on a study of the  $\beta$ -decay of  $^{56}\text{Cu}$  which, to our knowledge, represents the first successful attempt to investigate this decay. After a description of the experimental techniques in Section 2, we present the results of the measurements in Section 3, and discuss them in comparison with shell-model predictions in Section 4. Section 5 contains summary and outlook.

## 2. Experimental techniques

$^{56}\text{Cu}$  was produced by means of fusion-evaporation reactions between a 148 MeV  $^{32}\text{S}$  beam, delivered by the heavy-ion accelerator UNILAC of GSI Darmstadt, and a 2 mg/cm<sup>2</sup>  $^{\text{nat}}\text{Si}$  target. By using a FEBIAD–B2–C [9] or FEBIAD–E ion source [10], a mass-separated  $A = 56$  beam was prepared at the ISOL facility [11]. The intensity of the  $^{56}\text{Cu}$  beam amounted to about 1 atom/s for the FEBIAD–E source. This value was a factor 4 to 5 higher than that obtained for the FEBIAD–B2–C source. The  $A = 56$  beam contained  $^{56}\text{Co}$  and  $^{56}\text{Ni}$  contaminants, whose intensity were considerably higher than that of  $^{56}\text{Cu}$ . This reflects the dominance of the production cross-sections for  $^{28}\text{Si}(^{32}\text{S}, 3\text{pn})$  and  $^{28}\text{Si}(^{32}\text{S}, 2\text{p}2\text{n})$  reactions, respectively, over that for the  $^{28}\text{Si}(^{32}\text{S}, \text{p}3\text{n})$  reaction.

The mass-separated  $A = 56$  beam was implanted into a tape for the measurement of positrons and  $\beta$ -delayed  $\gamma$ -rays. The tape remained at rest for a preselected counting period and was subsequently transported away. During the counting period, the mass-56 beam was implanted either continuously (“grow-in measurement”) or during a limited collection time (“grow-in/decay measurement”). By choosing a sufficiently short cycle time, the  $A = 56$  contaminants were suppressed due to their long half-lives.

The implantation point was “viewed” by two  $\gamma$ -ray detectors (Ge single crystals) and a  $\beta$ -detector (plastic-scintillator). The total photopeak efficiencies of the Ge detectors were determined by using standard sources to be approximately 0.9% and 0.6%, respectively, for 1.3 MeV  $\gamma$ -rays. The efficiency of the scintillation detector was determined to be 46(4)% from a comparison of the photopeak intensities of  $^{58}\text{Cu}$   $\gamma$ -rays, measured by means of the Ge detectors

in singles as well as in coincidence with the  $\beta$ -detector. For this purpose a  $^{58}\text{Cu}$  beam, produced by  $^{32}\text{S} + ^{\text{nat}}\text{Si}$  or  $^{36}\text{Ar} + ^{\text{nat}}\text{Si}$  reactions in separate experiments, was implanted in the  $\beta\gamma$  detector array.

### 3. Experimental results

The relevant section of the  $\gamma$ -ray spectrum, measured for short-lived  $A = 56$  activity, is displayed in Fig. 1. These data were obtained by accumulating events from both  $\gamma$ -detectors in coincidence with signals from the plastic scintillator. The FEBIAD-B2-C source was used for  $5.4 \cdot 10^4$  grow-in cycles of 0.8 s each and  $5.2 \cdot 10^4$  grow-in/decay cycles of 0.3 s/0.5 s each, whereas the FEBIAD-E source was used for  $1.1 \cdot 10^4$  grow-in cycles of 0.8 s each. As can be seen from Fig. 1, there is no indication for contributions of the long-lived isobaric contaminants

$^{56}\text{Co}$  and  $^{56}\text{Ni}$ . Their suppression is due to the choice of short cycle times, with the detection of EC decay of  $^{56}\text{Ni}$  being prevented by the positron-coincidence condition.

The  $\gamma$ -lines at 1225.1(8), 2506.4(10), 2700.6(7) and 2782.5(20) keV, which are marked in Fig. 1 and compiled together with their intensities in Table 1, have been assigned to the  $\beta$ -decay of  $^{56}\text{Cu}$ . The most important arguments for this assignment are the firm mass determination, the short experimental half-life discussed below, and the agreement of the  $^{56}\text{Ni}$  level energies deduced from this work with reaction data [12] as well as with shell-model predictions. Before further evaluating these arguments, however, we want to present the measured properties of the four  $\gamma$ -transitions.

The  $\gamma$ -energy calibration was obtained by taking a  $\gamma$ -ray spectrum that contained both the new transitions and the well known  $\beta$ -delayed  $\gamma$ -rays of the

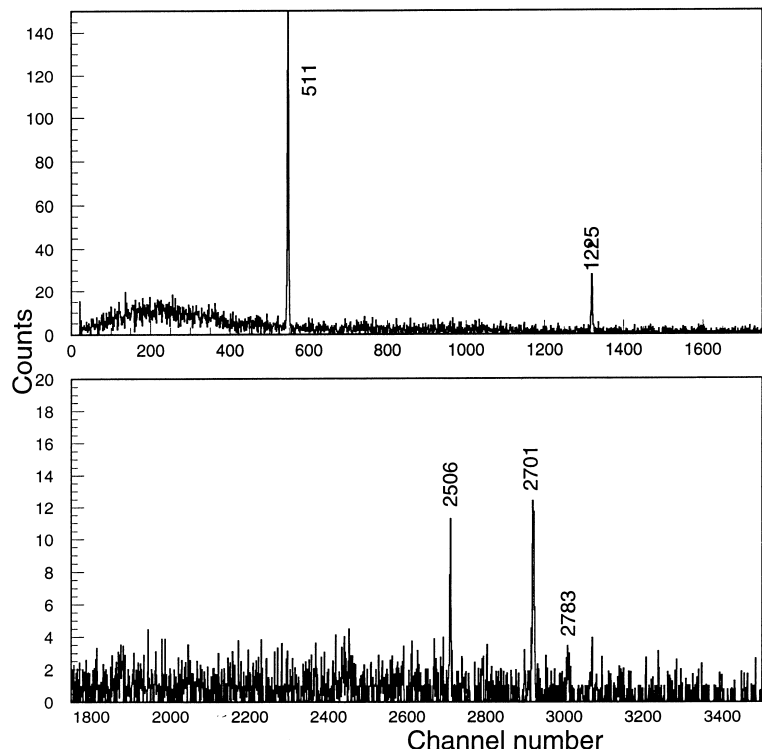


Fig. 1. Section of the  $\gamma$ -ray spectrum measured for  $A = 56$  sources in coincidence with the  $\beta$ -detector;  $\gamma$ -rays assigned to the  $\beta$ -decay of  $^{56}\text{Cu}$  are marked (see text).

Table 1

Experimental results for  $\beta$ -delayed  $\gamma$ -rays assigned to the decay of  $^{56}\text{Cu}$

$E_\gamma$ (keV)	$I_\gamma$ (%)
511	233(15)
1225.1(8)	77(9)
2506.4(10)	43(10)
2700.6(7)	100(13)
2782.5(20)	18(6)

isobaric contaminants  $^{56}\text{Co}$  and  $^{56}\text{Ni}$  [12]. For this purpose, grow-in cycles of about one hour were chosen. The  $\gamma$ -intensities were found by using the energy-dependent photopeak efficiency determined by means of standard sources. Intensity losses due to summation with coincident  $\gamma$ -rays, positrons or annihilation radiation were neglected, assuming that such losses would affect all  $\gamma$ -transitions in approximately

the same way. This approximation seems justified at the present level of accuracy of the  $\gamma$ -ray intensities (see Table 1). From the intensity balance based on the data compiled in Table 1, the  $\beta$ -feeding of the first excited  $2^+$  state of  $^{56}\text{Ni}$  turns out to be compatible with zero (5(17)%). We can indeed safely neglect this feeding since (i) the ground state of  $^{56}\text{Cu}$ , as a member of the  $T = 1$  triplet and mirror of  $^{56}\text{Co}$  ( $4^+$ ), can be assumed to have  $I^\pi = 4^+$ , and (ii) a  $\beta$ -decay to the first excited  $2^+$  state of  $^{56}\text{Ni}$  represented a second-forbidden non-unique transition with an lower log  $ft$  limit of 11.0 [13], which corresponded to an upper limit of  $9 \cdot 10^{-6}\%$  for the  $\beta$ -feeding. We therefore normalize the intensities of the remaining three  $\gamma$ -transitions to 100% and obtain the intensities listed in Table 1.

The half-life of  $^{56}\text{Cu}$  was determined to be 78(15) ms. This result represents an average of the values obtained by using  $\beta$ -coincident  $\gamma$ -data from the 0.8 s

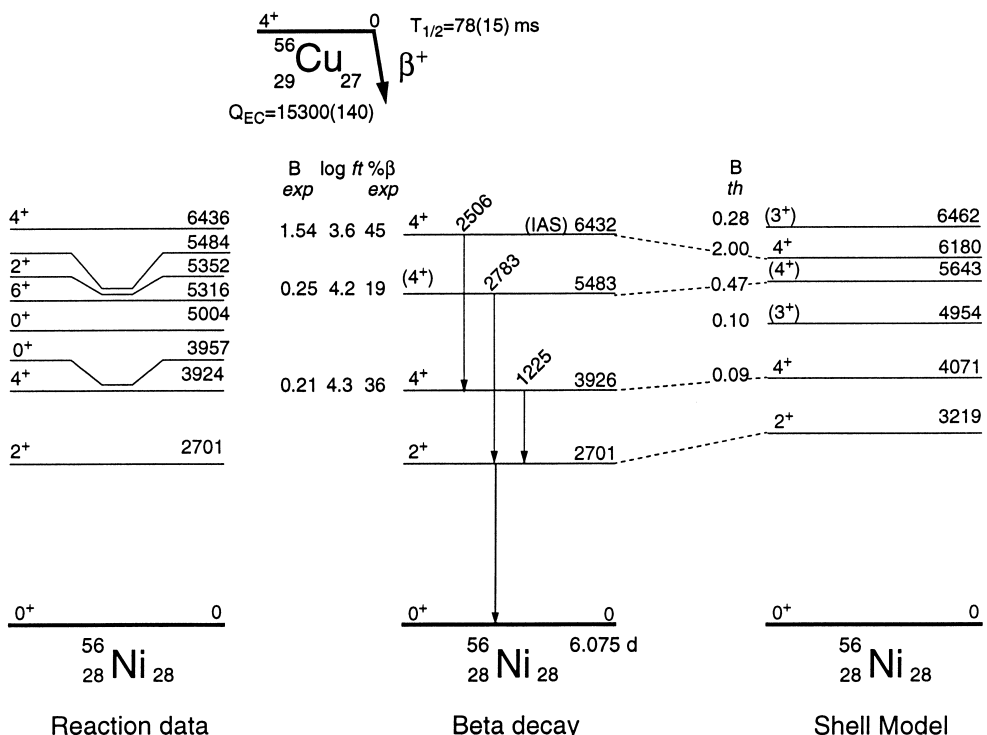


Fig. 2. Experimental results from the study of the  $\beta$ -decay of  $^{56}\text{Cu}$  in comparison with reaction data [12] and shell-model predictions. The experimental  $\beta$ -strength values  $B_{\exp}$  were deduced according to  $ft = 6177s/B_{\exp}$  for the IAS, and according to  $ft = 6177s/1.25^2B_{\exp}$  for the other  $^{56}\text{Ni}$  levels. In the case of the shell-model predictions, only the strongest transitions are shown, with  $^{56}\text{Ni}$  level energies stemming from Model C and  $\beta$ -strengths calculated from Model C plus the global effective GT operator (see text).

Table 2

Experimental  $\beta$ -decay data for low-lying  $^{56}\text{Ni}$  states. The level energies  $E_{\text{exp}}^{(\beta)}$ ,  $\beta$ -intensities  $I_{\beta}$ ,  $\log ft$  values, and  $\beta$ -strengths  $B(GT)_{\text{exp}}$ , determined in this work, are confronted to level energies  $E_{\text{exp}}^{(\text{react})}$  and spin/partiy assignments deduced in general from reaction data [12], and to level energies  $E_{\text{theor}}$  and  $\beta$ -strengths  $B(GT)_{\text{theor}}$  obtained from calculations based on Model A, B and C. The experimental  $\beta$ -strength values  $B(GT)_{\text{exp}}$  were deduced according to  $ft = 6177s/[B(F) + 1.25^2B(GT)_{\text{exp}}]$  by taking the theoretical value of  $B(F) = 2$  for the IAS and assuming pure GT transitions for the other  $^{56}\text{Ni}$  levels. In the case of the shell-model results, only the transitions corresponding to the strongest  $\beta$ -branchings are included (see text). The  $E_{\text{theor}}$  values stem from Model C. The theoretical values  $B(GT)_{\text{theory}} = B(GT)_{\text{eff}}$  were calculated by using the global effective GT operator (see text)

$E_{\text{exp}}^{(\beta)}$ (keV)	$E_{\text{exp}}^{(\text{react})}$ (keV)	$E_{\text{theor}}$ (keV)	$I^{\pi,T}$	$I_{\text{exp}}^{(\beta)}$ (%)	$\log ft_{\text{exp}}$	$B(GT)_{\text{exp}}$	$B(GT)_{\text{theory}}$		
							C	B	A
2700.6(7)	2700.6(7)	3219	$2^+,0$	—	—	—	—	—	—
3925.7(12)	3923.6(13)	4071	$4^+,0$	36(14)	4.3(2)	0.21(9)	0.09	0.13	0.72
—	—	4954	$(3^+),0$	—	—	—	0.10	0.23	0.07
5483.1(21)	5483.7(13)	5643	$(4^+),0$ <sup>a)</sup>	19(6)	4.2(2)	0.25(9)	0.47	0.50	0.21
6432.1(15)	6436(3)	6180	$4^+,1$	45(10)	3.6(1)	-0.29(26)	0.00	0.00	0.05
—	—	6462	$(3^+),1$	—	—	—	0.28	0.53	0.42

<sup>a)</sup> No spin/partiy assignment given from reaction data; however, a tentative  $4^+$  assignment can be deduced from a comparison with shell-model predictions (see text)

grow-in and 0.3 s/0.5 s grow-in/decay cycles mentioned above. The experimental  $^{56}\text{Cu} \rightarrow {}^{56}\text{Ni}$  decay scheme, deduced from this work is displayed in Fig. 2. The experimental  $\log ft_{\text{exp}}$  data, shown in Fig. 2 and Table 2, were determined by using half-life and branching-ratio results from this work and a  $Q_{EC}$  value of 15300(140) keV [6].

#### 4. Discussion

The  $^{56}\text{Ni}$  level energies deduced from this work agree with those determined by reaction experiments [12], but are more accurate for the isobaric analogue state (IAS), the uncertainty being reduced compared to the reaction data by a factor of 2 (see Table 2). The spin/partiy assignments from reaction work are confirmed for three of the four levels. The 5483 keV state, for which no spin/partiy assignment has been given so far, can be tentatively identified to be  $4^+$  on the basis of a comparison to shell-model predictions which will be presented in the following.

Within the framework of the simplest shell-model approach (Model A), the wave function for the ground state of  $^{56}\text{Cu}$  is the particle-hole configuration  $[(f_{7/2})^{-1} \times p_{3/2}](4^+, T=1)$ . It is connected by the GT operator to ten states in  $^{56}\text{Ni}$  with the particle-hole configurations  $[(f_{7/2})^{-1} \times p_{3/2}](3^+, 4^+,$

$5^+; T=0,1)$  and  $[(f_{7/2})^{-1} \times p_{1/2}](3^+, 4^+; T=0,1)$ , whereas GT transitions to the particle-hole states  $[(f_{7/2})^{-1} \times f_{5/2}]$  are  $\ell$ -forbidden. The largest GT strength for these 1p–1h transitions is  $B(GT)_{\text{free}} = 1.31$  for  $[(f_{7/2})^{-1} \times p_{3/2}](4^+, T=1) \rightarrow [(f_{7/2})^{-1} \times p_{3/2}](4^+, T=0)$ , where there are two components  $f_{7/2} \rightarrow f_{7/2}$  and  $p_{3/2} \rightarrow p_{3/2}$  which are in phase (the subscript "free" indicates that the free-nucleon  $\beta$ -decay operator is used). This is also the lowest-lying  $^{56}\text{Ni}$  state populated by allowed  $\beta$ -decay. The  $B(GT)_{\text{free}}$  value for the IAS is small because the two components are out of phase, and the Fermi strength is  $B(F) = 2$ . The total GT strength to all  $^{56}\text{Ni}$  states is 4.29, but most of this resides in states at higher excitation energy which are difficult to observe in  $\beta$ -decay experiments due to the small phase space. Thus, in Model A the  $\beta$ -decay is dominated by strong transitions to the  $4^+$   $T=0$  and  $T=1$  states.

Configuration mixing between these particle-hole states was included by using the FPD6\* interaction (Model B) which is the FPD6 interaction introduced by Richter et al. [14] with the single-particle energies modified to reproduce the experimental  $A = 55$  and  $A = 57$  single-particle properties, when the  $fp$  model space is truncated to the  $(f_{7/2})^{16}$  configuration [1]. The result of this mixing is that the transition strength to the lowest  $4^+$ ,  $T=0$  state is reduced from 1.31 to 0.23 due to interference with the smaller admixed

components. The total GT strength, summed over all  $^{56}\text{Ni}$  states, is the same as in Model A.

Finally we have extended the Model B calculations by including up to three particles excited from the  $f_{7/2}$  orbital to the  $p_{3/2}$ ,  $p_{1/2}$  and  $f_{5/2}$  orbitals (Model C). This model space includes the RPA-type correlations (2p–2h admixtures in the  $^{56}\text{Ni}$  ground state) which are important for quenching the GT strength within the  $fp$ -shell model space [15]. Indeed, the total GT strength calculated by using Model C is reduced by about a factor of two compared to the 1p–1h truncation (Model B). The excitation energies of  $T=1$  yrast states in  $^{56}\text{Co}$ , calculated on the basis of Model C, are in excellent agreement with the recent result deduced from in-beam  $\gamma$ -ray work [23].

The formalism for the  $\beta$ -decay calculations is given in Ref. [16]. To an accuracy of a few percent the more exact results from the formalism of Ref. [16] are given by  $ft = 6177s/[B(F) + (g_A/g_V)^2 B(GT)]$  where  $|g_A/g_V| = 1.25$ . Unlike the  $B(GT)$  values defined in Ref. [16], which implicitly included the  $(g_A/g_V)^2$  factor, the  $B(GT)$  results presented in this work do not include this factor (it appears explicitly in the equation for  $ft$  shown above) and are normalized such that  $B(GT)_{free} = 3$  for the neutron to proton decay ( $B(F) = 1$  for the neutron to proton decay). In addition, we have used the effective GT matrix elements of Martinez-Pinedo et al. [17], given by  $B(GT)_{eff} = (1 + \delta)^2 B(GT)_{free}$ , where  $\delta = -0.256$ , as determined from GT  $\beta$ -decay data in the lower  $fp$  shell. This value for  $\delta$  is close to the average value of  $\delta = -0.23$  obtained for the sd shell [16]. By comparison with magnetic moment data and the calculations performed by Towner [18] and Arima et al. [19], it has been deduced [20,21] that about 2/3 of this “global quenching” comes from higher-order configuration mixing and about 1/3 from  $\Delta$ -particle admixtures. The total strength obtained in Models A and B with the effective GT operator is 2.37.

Model C, including the global effective operator, was tested by calculating the  $\beta$ -decays of  $^{55}\text{Ni}$  and  $^{57}\text{Cu}$ . These decays are dominated by a nearly 100% branching to the ground state of the respective daughter nucleus [22], the shell-model transition densities being mainly  $f_{7/2} \rightarrow f_{7/2}$  and  $p_{3/2} \rightarrow p_{3/2}$ , respectively. The single-particle (Model A) matrix

elements for these two decays are 1.29 and 1.67, respectively. The results from Model C with the global effective operator are 0.39 and 0.19, respectively. The  $B(GT)$  values extracted from the experimental  $ft$  values [22] (with  $B(F) = 1$ ) are about 0.20 and 0.22, respectively. The agreement between experiment and theory is not perfect, but the small experimental  $B(GT)$  values confirm the importance of  $fp$ -shell configuration mixing and the global quenching.

The experimental and theoretical  $\beta$ -transition strengths for the  $^{56}\text{Cu}$  decay are compared in Table 2 and Fig. 2. The experimental  $B(GT)$  value for the IAS is obtained from the  $ft$  value after subtracting the  $B(F)$  value of 2. This results in a  $B(GT)_{exp}$  which is negative but consistent with zero within the experimental uncertainty. In the comparison, displayed in Table 2 and Fig. 2, only the strongest calculated transitions below 6.5 MeV in excitation have been taken into account, i.e. those with  $\log ft_{theor}$  values below 4.7 corresponding to branching ratios above 7%. The compilation of Table 2 does not include three  $^{56}\text{Ni}$  states predicted below 6.5 MeV with  $B(GT)_{eff}$  values lower than 0.01 at 5959 keV ( $5^+, 0$ ), 6048 keV ( $4^+, 0$ ), and 6356 keV ( $3^+, 0$ ). (The total additional  $B(GT)_{eff}$  strength above 6.5 MeV is 0.90, 0.98 and 0.17 in Models A, B and C, repectively.) The  $B(GT)$  values for the  $T=0$  final states, in particular to the lowest two  $4^+$  states, provide a sensitive test of the residual particle-hole interaction in a situation where the configurations are relatively simple. The  $B(GT)_{eff}$  value from Model C, including the global effective operator, is small compared to experiment for the first  $4^+$   $T=0$  state and is large compared to experiment for the second  $4^+$   $T=0$  state. However, the experimental uncertainties are rather large, and more accurate half-life and branching ratio measurements are required for a more stringent comparison.

It has recently become possible to carry out full  $fp$  shell calculations for  $^{56}\text{Ni}$  with the Quantum Monte Carlo Diagonalization method [5], where it was found that the low-lying spectrum of  $^{56}\text{Ni}$  was in reasonable agreement with the FPD6 interaction. Hopefully this method can be used in the near future to calculate the  $\beta$ -decay of  $^{56}\text{Cu}$ . We note that the component of the closed-shell ( $f_{7/2})^{16}$  configuration in the  $^{56}\text{Ni}$  ground state is 71% in our Model C and

53% [5] in the full-*fp* model space. Although the configuration mixing is large, the simple “quasiparticle” single-particle states and 1p–1h excitations are still identifiable in the calculations and can thus be compared to experiment [1,2].

## 5. Summary and conclusion

We performed a “pilot” study of the  $^{56}\text{Cu}$   $\beta$ -decay. Four  $\beta$ -delayed  $\gamma$ -rays were assigned to this decay, and its half-life was determined to be 78(15) ms. The resulting  $B(GT)$  values are interpreted with reference to shell-model calculations. The limited quality of the experimental data allows for only qualitative conclusions. However, with the production method and the “gross properties” of  $^{56}\text{Cu}$  being known from this experiment, the stage is set now for more refined studies.

## Acknowledgements

This work was supported in part by GSI Darmstadt, IN2P3 (Institut National de Physique Nucléaire et de Physique des Particules), the Polish Committee of Scientific Research under grant KBN 2 P03B 039 13, and the European Community under contract No. ERBFMGECT950083. B.A.B. would like to acknowledge the support by the Alexander von Humboldt-Foundation and NSF grant 9605207. W.L. wishes to thank the Deutscher Akademischer Aus-

tauschdienst and the Hongkong Qiushi Science Foundation for support.

## References

- [1] G. Kraus et al., Phys. Rev. Lett. 73 (1994) 1773.
- [2] K.E. Rehm et al., Phys. Rev. Lett. 80 (1998) 676.
- [3] X.G. Zhou et al., Phys. Rev. C 53 (1996) 982.
- [4] S.E. Koonin, D.J. Dean, K. Langanke, Phys. Rep. 278 (1997) 1.
- [5] T. Otsuka, M. Honma, T. Mizusaki, Phys. Rev. Lett., to be published.
- [6] G. Audi et al., Nucl. Phys. A 624 (1997) 1.
- [7] W.E. Ormand, Phys. Rev. C 55 (1997) 2407.
- [8] F. Pougeon et al., Z. Phys. A 327 (1987) 17.
- [9] R. Kirchner et al., Nucl. Instr. and Meth. Phys. Res. A 234 (1985) 224.
- [10] R. Kirchner et al., Nucl. Instr. and Meth. Phys. Res. 186 (1981) 295.
- [11] K. Burkard et al., Nucl. Instr. and Meth. Phys. Res. B 126 (1997) 12.
- [12] J. Huo, Nucl. Data Sheets 67 (1992) 523.
- [13] S. Raman, N.B. Gove, Phys. Rev. C 7 (1973) 2008.
- [14] A. Richter et al., Nucl. Phys. A 523 (1991) 325.
- [15] N. Auerbach et al., Nucl. Phys. A556 (1993) 190.
- [16] B.A. Brown, B.H. Wildenthal, At. Data, Nucl. Data Tables 33 (1985) 347.
- [17] G. Martinez-Pinedo et al., Phys. Rev. C 53 (1996) R2602.
- [18] I.S. Towner, Phys. Rep. 155 (1987) 264.
- [19] A. Arima et al., Adv. Nucl. Phys. 18 (1987) 1.
- [20] B.A. Brown, B.H. Wildenthal, Ann. Rev. Nucl. Part. Sci. 38 (1988) 29.
- [21] B.A. Brown, B.H. Wildenthal, Nucl. Phys. A 474 (1987) 290.
- [22] R.B. Firestone et al., Table of Isotopes (Wiley Interscience Publication, 1996).
- [23] M. Palacz et al., Nucl. Phys. A 627 (1997) 162.